

1/25/95  
E9178

NASA TM 106756

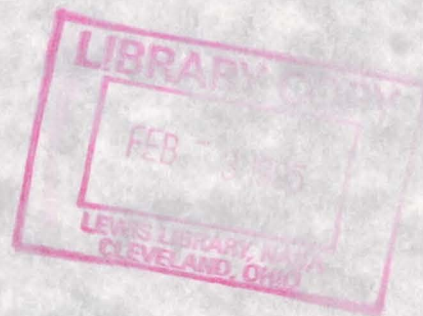
NASA Technical Memorandum 106756

# Bending Properties of Nickel Electrodes for Nickel-Hydrogen Batteries

Brad A. Lerch and Richard M. Wilson  
*National Aeronautics and Space Administration  
Lewis Research Center  
Cleveland, Ohio*

Dennis Keller  
*Real World Quality Systems, Inc.  
Rocky River, Ohio*

Ralph Corner  
*NYMA, Inc.  
Engineering Services Division  
Brook Park, Ohio*



January 1995



National Aeronautics and  
Space Administration

## BENDING PROPERTIES OF NICKEL ELECTRODES FOR NICKEL-HYDROGEN BATTERIES

Brad A. Lerch and Richard M. Wilson  
National Aeronautics and Space Administration  
Lewis Research Center  
Cleveland, Ohio 44135

Dennis Keller  
Real World Quality Systems, Inc.  
Rocky River, Ohio 44116

and

Ralph Corner  
NYMA, Inc.  
Engineering Services Division  
Brook Park, Ohio 44142

### SUMMARY

Recent changes in manufacturing have resulted in nickel-hydrogen batteries that fail prematurely by electrical shorting. This failure is believed to be a result of a blistering problem in the nickel electrodes. In this study the bending properties of nickel electrodes are investigated in an attempt to correlate the bending properties of the electrode with its propensity to blister. Nickel electrodes from three different batches of material were tested in both the as-received and impregnated forms. The effects of specimen curvature and position within the electrode on the bending strength were studied, and within-electrode and batch-to-batch variations were addressed. Two color-imaging techniques were employed to differentiate between the phases within the electrodes. These techniques aided in distinguishing the relative amounts of nickel hydroxide surface loading on each electrode, thereby relating surface loading to bend strength. Bend strength was found to increase with the amount of surface loading.

### INTRODUCTION

Nickel-hydrogen batteries are used to store energy in satellites. Future plans are to use them in the International Space Station Alpha. The batteries consist of alternate nickel and hydrogen electrodes, gas screens, and a separator sandwiched around a central core in a pressure vessel container. The nickel electrodes, which are manufactured by sintering nickel powder onto a nickel-wire mesh, are porous structures (approximately 80-percent porosity), with a typical cross section as shown in figure 1. The sintered electrode is electrochemically impregnated with active nickel hydroxide ( $\text{Ni}(\text{OH})_2$ ). Recent changes in manufacturing have resulted in Ni electrodes that "blister" during service. After a blister forms, it subsequently spalls, sometimes reaching the hydrogen electrode and shorting the electrode stack. The blistering is believed to occur because the electrodes were sintered too long and a more continuous, fused layer of nickel (i.e., less porous) was formed near the surfaces of the electrodes. This layer restricts the  $\text{Ni}(\text{OH})_2$  from penetrating the full thickness of the electrode during impregnation, and thus, the  $\text{Ni}(\text{OH})_2$  is concentrated near the surface. This is called surface loading. Surface loading can contribute to a number of undesirable events such as lowering the active material utilization and the ampere-hour capability; trapping the acidic impregnation solution in the electrode pores, which causes additional corrosion of the nickel-wire mesh support structure and thus further weakens the sinter; and generating oxygen at the nickel electrode during overcharging. In the latter case, as oxygen gas is generated within the electrode, surface loading is believed to prevent the gas from escaping. The gas pressure builds internally, pushing on the contiguous, surface-loaded layer until blistering occurs.

The surface-loaded layer, being more dense than the rest of the electrode, should be stronger than the more porous layers in a "good" electrode. A bend test, which concentrates the applied stresses in the surface layers, may be useful in differentiating between electrodes with and without surface loading. If bending strength, or some other mechanical property, could be correlated with surface loading, such a test could be used in quality control, allowing only electrodes with a

minimum propensity to blister to be put into service. Bend tests may also be useful in monitoring electrode or batch uniformity, providing a quality control check on the manufacturing process. The study reported herein was meant to be a first-cut investigation into the bending properties of Ni electrodes and to provide a basis for follow-on studies.

## MATERIAL

Three batches of Ni electrodes were supplied in both the as-sintered and impregnated forms. These batches represent electrodes (1) from a baseline design (batch B); (2) from an improved design (batch A); and (3) from an optimized manufacturing process that produced a more uniformly sintered product (batch C). Three electrodes per batch were tested. As-sintered electrodes were flat squares as shown in figure 2, parts (a) to (c). The impregnated electrodes were flat rounds (fig. 2(d)).

Specimens were taken from the electrodes as indicated in figure 2. The specimens were thin strips, nominally 7 mm wide by 70 mm long by 0.78 mm thick. A razor blade was used to cut the specimens from the electrodes, with the long axis of the specimen parallel to one set of wires in the Ni-wire mesh. Ten samples were sectioned from as-sintered electrode s/n 100 (serial number 100) of batch A. Usually, four specimens were sectioned from each of the other electrodes. The test matrix is shown in figure 3.

## THREE-POINT BEND TESTS

Three-point bend tests were run according to ASTM Standard E855—"Bend Testing of Metallic Flat Materials for Spring Applications Involving Static Loading." It should be noted, however, that the specimen dimensions did not comply with the standard, but we were limited by the physical dimensions of the electrodes. Also, an existing three-point bend fixture, which was used for the tests, possessed 4.7-mm-diameter rollers for the contact support points and load applicator rather than the knife edges recommended in the standard. A 40-mm span was employed in the bend tests; a schematic of the test fixture is shown in figure 4. Specimen deflection at midspan was inferred from machine crosshead displacement, with no correction for the stiffness of the load frame. We believed that no corrections were needed because the stiffness of the specimens was much less than that of the load frame. The bend tests were run at a constant crosshead displacement of 0.05 in./min. Load-displacement diagrams were plotted for each specimen, and the following data were calculated from these curves: elastic modulus  $E_b$ ; displacement at maximum load  $\delta_p$ ; and bending strength  $\sigma_p$ . These quantities are indicated in a typical load-displacement diagram in figure 5. The elastic modulus was obtained by determining the slope of the straight portion of the curve (i.e., the initial load-displacement points) and using the following equation:

$$E_b = PL^3/4bh^3\delta \quad (1)$$

where

- P load increment
- L span length between supports (40 mm)
- b specimen width (nominally 7 mm)
- h specimen thickness (nominally 0.78 mm)
- $\delta$  deflection at midspan

The maximum bending strength was obtained as follows:

$$\sigma_p^1 = 1.5P_pL/bh^2 \quad (2)$$

where  $P_p$  is the maximum load.

Equation (2) is derived from plate theory; however, the specimens used in this study are better represented by beams. The maximum bending strength from beam theory is given by

$$\sigma_p^2 = 2P_pL/bh^2 \quad (3)$$

Equation (3) is not given in ASTM Standard E855.

Both the beam theory and plate theory values for maximum bending strength are listed in tables I and II, along with the elastic modulus and the displacement at maximum load. Since equations (2) and (3) differ only by a constant, we arbitrarily decided to use the results from equation (2) in subsequent analyses. Only the absolute values, not the trends, were changed by using values from equation (3).

## RESULTS

The two curves plotted in figure 6 show a large difference between the bending behavior of the as-sintered and impregnated electrodes. The as-sintered samples were significantly less stiff and were weaker than the impregnated samples. In addition, the impregnated samples reach their maximum strength at a lower displacement  $\delta_p$ . The mean values of bending strength and initial modulus are summarized in table III.

Several analyses of variance were performed on the bending strengths (as calculated by eq.(2)) to investigate the effect of different factors and components on the variance. The following sections address these analyses.

### Effect of Specimen Curvature

After the specimen was cut from the electrode, the specimen was left with a slight curvature along its length (similar to that shown in fig. 4). To check if the curvature had an effect on the bending strength, five specimens from electrode s/n 100 (batch A, as-sintered) were tested in the curve-up position, and the other five in the curve-down position. Statistical analysis indicated that there was no significant difference between the curve-up and curve-down configurations. For convenience, all of the remaining specimens in this study were tested in the curve-down position (as shown in fig. 4).

### Effect of Specimen Position Within the Electrode

Hanging electrodes were impregnated in an electrolytic bath, the design of which made it possible for the bottom of the electrode to be more heavily impregnated than the top. Thus, a positional difference may have been manifested in the resulting bend strengths. To test this hypothesis, two specimens were taken from the top and two from the bottom of each electrode (fig. 2). The mean bending strengths are given on a per batch basis in table IV. Statistical analysis of the data showed no significant strength difference between the top and bottom of the as-sintered batch A electrodes. The other two batches (batches B and C), however, were found to have small, but statistically significant, differences in strength between the top and the bottom in the as-sintered condition: the bottom was stronger. The small differences in bend strength could be detected because of good test-to-test reproducibility (see  $S_{\text{specimen}}$  in table IV). After impregnation, the bending strengths of specimens taken from the bottom of the electrodes were often higher than those taken from the top. However, there was no statistically significant strength difference between the top and bottom of the electrode for any of the three batches. The inability to detect statistically significant positional differences in the impregnated electrodes was due to the large increase in test-to-test variation (see  $S_{\text{specimen}}$  in table IV).

### Strength Variation

This section addresses the bending strength variation in the electrodes.

Variation level 1: Within electrode.—*Within* a given electrode, the 95-percent confidence variations about the mean were

As-sintered:  $\pm 1.95$  MPa

Impregnated:  $\pm 6.30$  MPa

These numbers include positional (i.e., top-to-bottom) and test-to-test variation.

Variation level 2: Within batch.—Significant electrode-to-electrode variation within a batch was discernible over and above the within-electrode variation. The within-batch 95-percent confidence variations about the mean were

As-sintered:  $\pm 2.45$  MPa

Impregnated:  $\pm 7.99$  MPa

These numbers include electrode-to-electrode, positional (i.e., top to bottom), and test-to-test variation. These values, therefore, represent the variation that can be expected by testing a random electrode in the future.

#### Differences in Mean Bending Strength Among Batches

At the 99.9-percent confidence level, statistical analysis showed significant differences among the mean bending strengths of the as-sintered electrodes in the batches (table III): from strongest to weakest they were batch B, batch C, and batch A. This difference, however, was moderated by impregnation. After impregnation, only batch B had a marginally significant (90-percent confidence) strength increase over batch A, and batch C was not significantly different from either batch A or B. This moderation was due to the larger within-batch variation in the impregnated material.

#### METALLOGRAPHY

To aid in the analysis of the mechanical properties, metallographic sections were taken from selected electrodes. Two color-imaging techniques were employed to demonstrate phase distribution in the Ni electrodes. By using these techniques, we could readily determine the extent of surface loading and Ni-powder distribution on metallographic sections taken from the electrodes. Such a determination is not possible with black and white imaging. The first technique employs color coding of back-scattered electron (BSE) images taken with a scanning electron microscope (SEM). This technique yields the largest contrast difference between phases and allows information to be easily acquired. However, this technique requires an SEM and image analysis capabilities, and it is inherently time consuming. The second technique, an interference-layering method, is faster and less expensive. However, the color contrast is poorer than that obtained from the SEM method, and thus, differentiation between phases is more difficult.

#### INTERFERENCE-LAYERED REACTIVE SPUTTERING

A surface layer of  $\text{PtO}_2$  was sputtered onto polished metallographic sections of the electrodes. The sputtering was performed with a Pt target 2 cm above the sample surface. The sputtering chamber was backfilled with 1 mbar oxygen. A bias voltage of 650 V and a current of 55 mA was applied for 265 sec. Additional details of the process can be found in reference 1. This technique accentuates the contrast differences between different phases. The particular colors that form and the magnitude of the contrast depend on the optical constants of the phases in the substrate and in the  $\text{PtO}_2$  layer. A detailed explanation of this effect can be found in reference 2.

Bright field micrographs of a typical interference-layered electrode are shown in figure 7. The light-colored phase is the epoxy mounting material; the rose-colored phase is the Ni powder and the Ni-wire mesh; the brown phase is the  $\text{Ni(OH)}_2$ ; and the black areas are voids that were not filled with epoxy. The surface loading is easily seen in figure 7(a) as the darker layer near each surface of the electrode. There is much less  $\text{Ni(OH)}_2$  at the mid-thickness of the electrode. However, most of the Ni powder throughout the electrode cross section appears to have been coated with  $\text{Ni(OH)}_2$ , since most of the rose-colored particles in figure 7(b) are surrounded by the brown  $\text{Ni(OH)}_2$ . The Ni-wire mesh, conversely, does not appear to have been wetted by the  $\text{Ni(OH)}_2$ .

#### BACK-SCATTERED SEM IMAGES

BSE images were taken of polished metallographic sections. Depending on its average atomic number, each phase in the electrode produced a different electron intensity, which could be assigned a specific color through an image analyzer.

The phases were given the following colors:

Red	Ni powder and wire mesh
Blue	Ni(OH) <sub>2</sub>
Green	epoxy or voids

Figure 8 shows a cross section of a typical as-sintered electrode. In all batches, the Ni powder was uniformly distributed, and the particles were isolated from one another. No continuous, fused layer was observed at the surfaces in any of the batches of electrodes.

Figure 9 is a color-coded BSE image taken from batch A impregnated electrode s/n 202. Figure 9(a) shows a specimen taken from the top of the electrode (bend specimen #21), and figure 9(b) shows one from the bottom of the electrode (bend specimen #23). There is a much more uniform distribution of Ni(OH)<sub>2</sub> (blue phase) in the top of the electrode (fig. 9(a)) compared to the bottom (fig. 9(b)), where the blue is concentrated near the electrode surfaces (i.e., surface loading). This concentration of Ni(OH)<sub>2</sub> is believed to have strengthened specimens taken from the bottom of the electrode, as evidenced by the higher bending strength of specimen #23 (16.9 MPa) compared to specimen #21 (14.5 MPa) in batch A.

A similar occurrence was observed in batch A impregnated electrode s/n 200; specimens taken from the top of the electrode (fig. 10(a)) had less surface loading than specimens taken from the bottom (fig. 10(b)). This again resulted in a higher strength for specimens taken from the bottom of the electrode. A comparison of figures 9 and 10 indicates that the amounts of surface loading in the bottom of electrode s/n 202 (fig. 9(b)) and the top of electrode s/n 200 (fig. 10(a)) are similar and likewise have similar bending strengths.

## DISCUSSION

Nickel electrodes were subjected to three-point bend tests in an effort to determine relative amounts of surface loading and the subsequent propensity of the electrodes to blister during service. Figures 9 and 10 show that there is a relationship between the bending strength and the amount of surface loading: the more surface loading, the higher the bend strength. These figures also explain why batch A impregnated electrode s/n 202 had a lower strength (and stiffness<sup>1</sup>) than the other electrodes in this batch; that is, it had less surface loading. Therefore, bend tests can be used as a screening test for surface loading.

The amount of surface loading within the electrode varies (at least in batch A), as evidenced in figures 9 and 10. This is believed to be due to various factors in the electrolytic impregnation setup. Further investigation into the specific impregnation process is required to remedy the nonuniformity between the top and bottom of the electrodes. Although this difference is manifested in the mechanical properties, the effects of this nonuniformity on the electrical properties have not been determined.

The initial theory attributing surface loading to over-sintering and the formation of a continuous, fused layer of Ni powder on the surfaces does not appear to hold. In figures 8 to 10 the Ni powder (red phase in these figures) appears to be distributed uniformly in both as-sintered and impregnated electrodes for all the batches. Furthermore, the Ni-powder particles are reasonably isolated from one another. Therefore, another explanation of the cause of surface loading is required. No connection has been proven in this study between the amount of surface loading and the propensity of the electrodes to blister. However, it should be pointed out that all of the batches showed surface loading, and all of the batches blistered when tested in the recirculating stack design.<sup>2</sup> This connection, if there is one, needs further study. It is interesting to note that the Ni-wire mesh is not wetted by the Ni(OH)<sub>2</sub>, and this could play a role in the blistering process.

---

<sup>1</sup>Although stiffness was not thoroughly examined, it is believed to follow trends similar to the bend strength.

<sup>2</sup>In this design the positive and negative electrodes alternate position in the electrode stack (i.e., +/-/-).

It has been industrial practice to bend test as-sintered electrodes for quality control purposes. This study has shown that the impregnation process results in a substantial change in both the mean bending strength (and stiffness) as well as the variability in strength. In addition, as shown by batch A, uniform as-sintered electrodes can develop nonuniformities (i.e., increased within-electrode variation) during impregnation. Therefore, testing as-sintered electrodes is not recommended as a predictor of electrode behavior because the electrode properties change drastically after impregnation.

#### SUMMARY OF RESULTS

Three-point bend tests were performed on three differently processed batches of both as-sintered and impregnated electrodes. Our findings were as follows:

1. The impregnated electrodes were stiffer and stronger than the as-sintered electrodes.
2. In batches B and C, there were small, but statistically significant, differences in bend strength between specimens taken from the top and the bottom of the as-sintered electrodes. The large variation amongst the impregnated specimens statistically obscured any positional differences in bending strength.
3. Two color-imaging techniques were developed to reveal surface loading and aid in phase analysis of the electrodes.
4. Bend tests can be used to determine relative amounts of surface loading; the more surface loading, the higher the bend strength.
5. Bend testing of as-sintered electrodes is not recommended as a predictor of electrode behavior since the properties drastically changed after impregnation.

#### ACKNOWLEDGMENT

The authors thank Ralph Pawlik for his assistance with the experiments.

#### REFERENCES

1. Interference-Layering Metallographic Technique Wins 1993 Jacquet-Lucas Award, Adv. Mater. Proc., vol. 145, no. 2, Feb. 1994, pp. 21-22.
2. Buehler, H.E.; and Hougardy, H.P.: Atlas of Interference Layer Metallography. Deutsche Gesellschaft fuer Metallkunde, Oberursel, W. Germany, 1980.

TABLE I.—BEND TEST RESULTS OF AS-SINTERED SPACE STATION BATTERY ELECTRODES

Serial number	Specimen number	Displacement at maximum load, $\delta_p$ , mm	Elastic modulus, $E_b$ , MPa	Maximum bending strength, MPa		Curvature	Figure
				Plate theory, $\sigma_p^1$ , MPa	Beam theory, $\sigma_p^2$ , MPa		
Batch A (84-percent porosity)							
100	1	3.34	1155	5.74	7.65	Down	2(a)
	2	4.02	1279	6.42	8.55	Up	
	3	3.51	1622	7.44	9.91	Down	
	4	5.29	1635	8.32	11.10	Up	
	5	2.58	1879	7.14	9.52	Down	
	6	3.60	1492	7.07	9.42	Up	
	7	3.55	1497	6.95	9.27	Down	
	8	4.02	1354	7.11	9.48	Up	
	9	3.30	1708	7.35	9.80	Down	
	10	3.81	1230	6.39	8.51	Up	
101	11	2.96	991	4.86	6.47	Down	2(c)
	12	3.47	1074	5.06	6.74		
	(12B)	3.30	1244	5.72	7.63		
	13	3.50	1141	5.51	7.35		
102	14	2.88	1164	5.04	6.72		
	21	3.38	1074	5.47	7.29		
	22	3.26	1115	5.38	7.17		
	(22B)	2.96	1139	5.23	6.97		
	23	2.88	1171	5.40	7.19		
24	3.26	1202	5.80	5.80	7.74		
Batch B (81-percent porosity)							
110	1	3.47	2356	8.96	11.95	Down	2(b)
	2	3.13	2253	9.85	13.13		
	3	3.85	2565	9.90	13.19		
	4	3.09	2727	10.32	13.76		
111	11	2.03	2302	8.08	10.77		
	12	2.54	2705	9.47	12.61		
	13	3.13	3295	12.02	16.02		
112	14	2.71	1917	10.32	13.75		
	21	2.54	2529	9.40	12.53		
	22	3.00	2475	9.84	13.12		
	23	3.38	1968	9.56	12.75		
	24	(a)	(a)		10.64	14.19	
Batch C (optimized plaque; 81-percent porosity)							
120	1	3.64	1524	7.08	9.43	Down	2(c)
	2	3.64	1510	7.25	9.66		
	(2B)	3.51	1405	6.52	8.69		
	3	3.89	1577	7.79	10.39		
121	4	3.93	1554	7.96	10.62		
	11	3.30	1628	7.44	9.92		
	12	3.81	1759	7.87	10.49		
122	13	4.53	1799	8.71	11.62		
	14	3.55	1583	7.90	10.53		
	21	3.17	1839	7.59	10.12		
	22	2.41	1750	7.77	10.36		
	23	3.72	1826	8.44	11.25		
	24	4.36	2056	9.87	9.87	13.15	

<sup>a</sup>No data—recorder error.



TABLE II.—BEND TEST RESULTS OF IMPREGNATED SPACE STATION BATTERY ELECTRODES

Serial number	Specimen number	Displacement at maximum load, $\delta_p$ , mm	Elastic modulus, $E_b$ , MPa	Maximum bending strength, MPa		Curvature	Figure		
				Plate theory, $\sigma_p^1$ , MPa	Beam theory, $\sigma_p^2$ , MPa				
Batch A (84-percent porosity)									
200	1	0.97	7 772	17.15	22.86	Down ↓	2(d) ↓		
	2	.93	8 535	19.76	26.35				
	3	1.14	9 448	22.12	29.49				
	4	1.10	12 165	25.35	33.80				
201	11	1.57	10 068	24.66	32.88				
	12	1.27	11 869	21.69	28.91				
	13	.85	13 096	20.47	27.29				
202	14	.85	13 454	20.85	27.79				
	21	1.48	5 470	14.53	19.37				
	22	1.57	5 153	14.71	19.61				
	23	1.31	6 252	16.88	22.50				
	24	1.52	7 985	17.18	22.91				
Batch B (81-percent porosity)									
210	1	1.86	6 998	21.36	28.47			Down ↓	2(d) ↓
	2	2.16	7 714	25.54	34.05				
	3	2.28	7 320	28.26	37.67				
	4	1.69	7 025	21.96	29.27				
211	11	1.99	6 975	22.30	29.73				
	12	1.86	9 180	23.84	31.78				
	13	1.95	8 869	25.98	34.64				
212	14	1.86	7 509	23.98	31.98				
	21	1.65	11 171	20.34	27.11				
	22	1.61	9 989	25.72	34.28				
	23	1.52	10 674	26.15	34.86				
	24	1.86	8 725	29.13	38.83				
Batch C (optimized plaque; 81-percent porosity)									
220	1	1.02	7 724	16.3	21.7	Down ↓	2(d) ↓		
	2	1.44	11 533	22.3	29.7				
	3	-----	9 999	-----	-----				
	4	5.84	9 779	22.9	30.5				
221	11	1.10	10 718	20.7	27.6				
	12	1.27	13 042	26.4	35.2				
	13	1.06	11 113	20.1	26.8				
	14	1.06	15 373	24.7	32.9				
222	21	-----	-----	20.4	27.2				
	22	1.23	10 351	19.3	25.6				
	23	1.57	9 461	22.2	29.6				
	24	1.27	8 026	18.7	25.0				

TABLE III.—MEAN VALUES OF BENDING STRENGTH AND MODULUS

	Mean bending strength, MPa	Mean elastic modulus, MPa
As-sintered electrodes		
<b>Total</b>	7.9	1 789
<b>Batch A</b>	5.9	1 253
Electrode 100	6.9	1 496
101	5.2	1 123
102	5.5	1 140
<b>Batch B</b>	9.9	2 422
Electrode 110	9.8	2 476
111	10.0	2 555
112	9.9	2 236
<b>Batch C</b>	7.9	1 692
Electrode 120	7.3	1 514
121	8.0	1 693
122	8.4	1 868
Impregnated electrodes		
<b>Total</b>	21.8	9 469
<b>Batch A</b>	19.6	9 273
Electrode 200	21.1	9 480
201	21.9	12 122
202	15.8	6 216
<b>Batch B</b>	24.5	8 511
Electrode 210	24.3	7 265
211	24.0	8 133
212	25.3	10 134
<b>Batch C</b>	21.4	10 623
Electrode 220	21.1	9 759
221	23.0	12 562
222	20.2	9 547

TABLE IV.—MEAN BENDING STRENGTH AS A FUNCTION OF POSITION IN THE ELECTRODE

	Mean bending strength, MPa		
	Batch A	Batch B	Batch C
As-sintered			
Top	5.96	9.27	7.36
Bottom	6.38	10.46	8.45
<sup>a</sup> S <sub>specimen</sub>	.48	.85	.49
Impregnated			
Top	18.75	23.18	20.90
Bottom	20.48	25.91	21.72
<sup>a</sup> S <sub>specimen</sub>	1.48	2.65	2.81

<sup>a</sup>Standard deviation among repeat tests within a position.

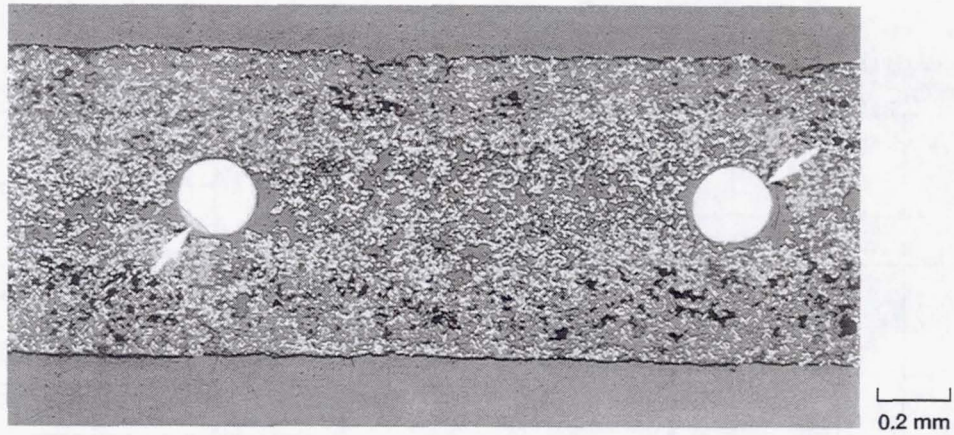


Figure 1.—Electrode cross section (arrows indicate Ni-wire mesh).

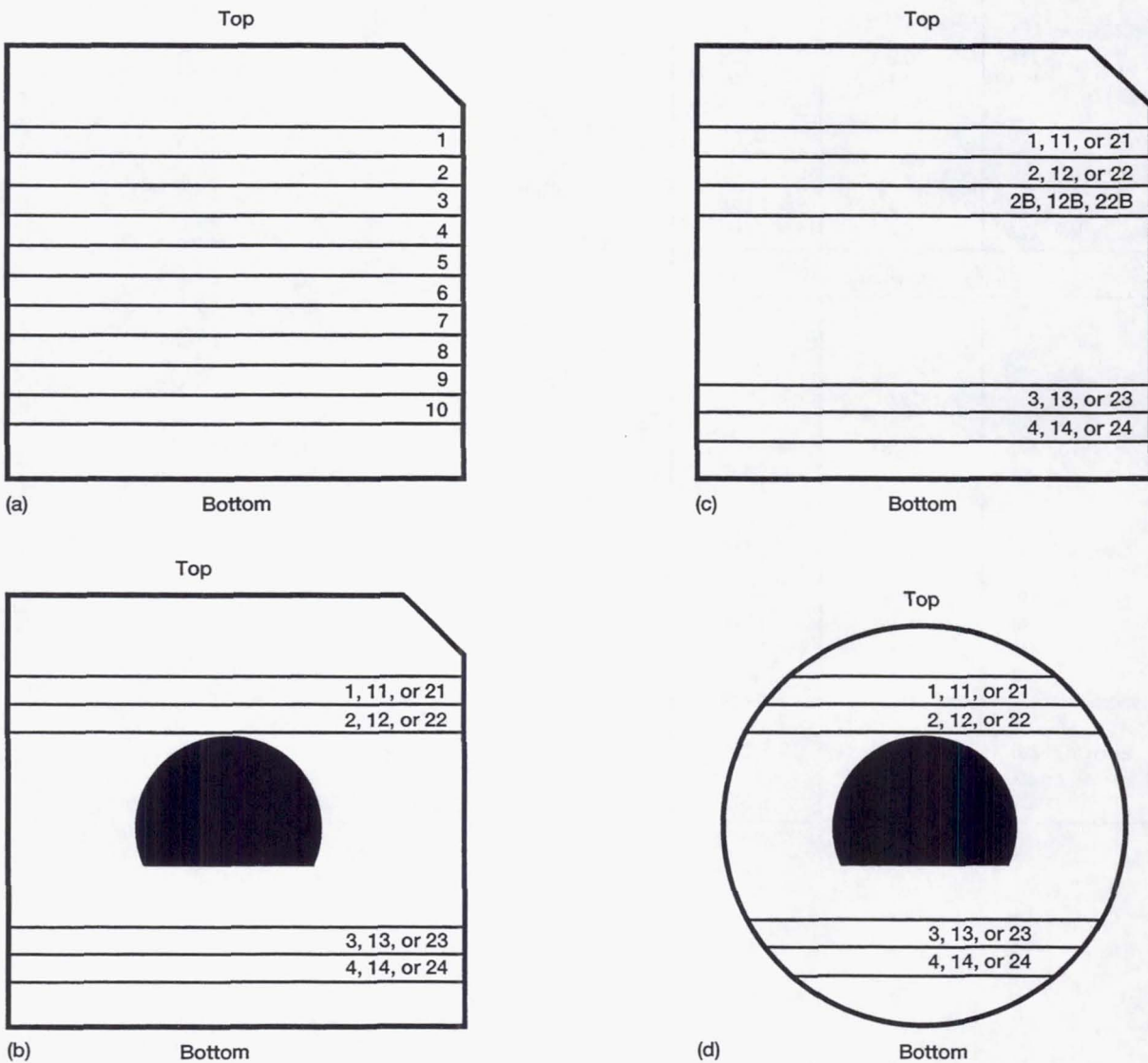


Figure 2.—Specimen location in electrodes. (a) to (c) As-sintered specimens. (d) Impregnated electrode specimens.

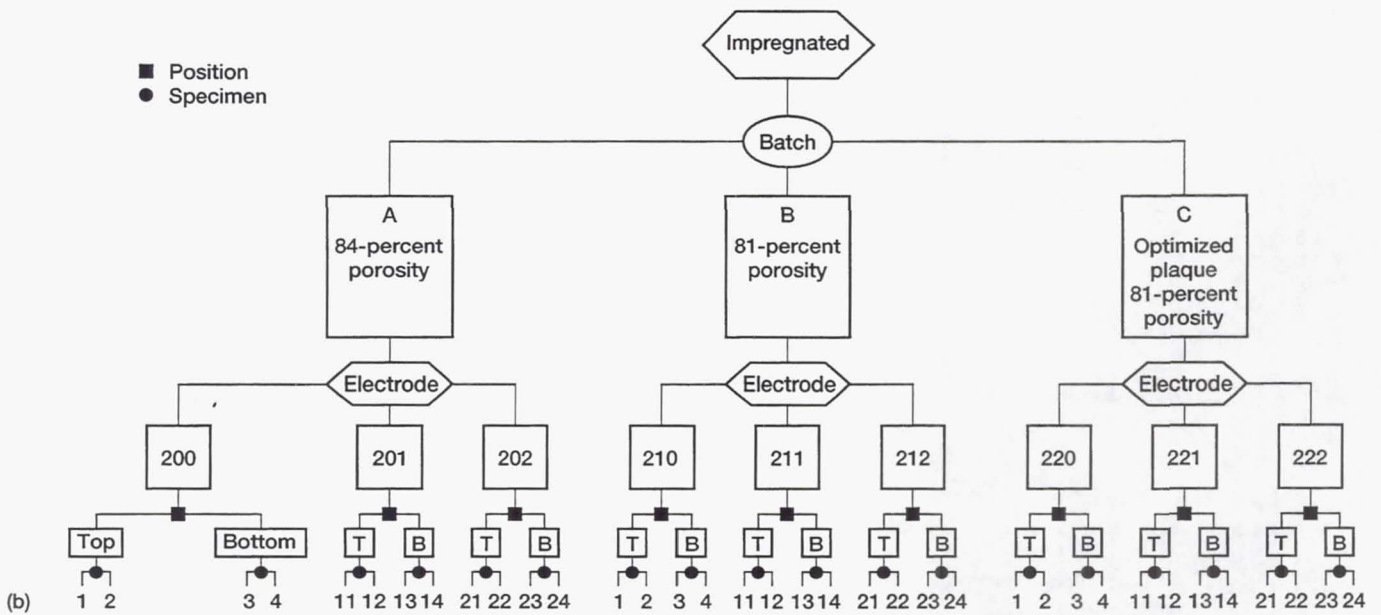
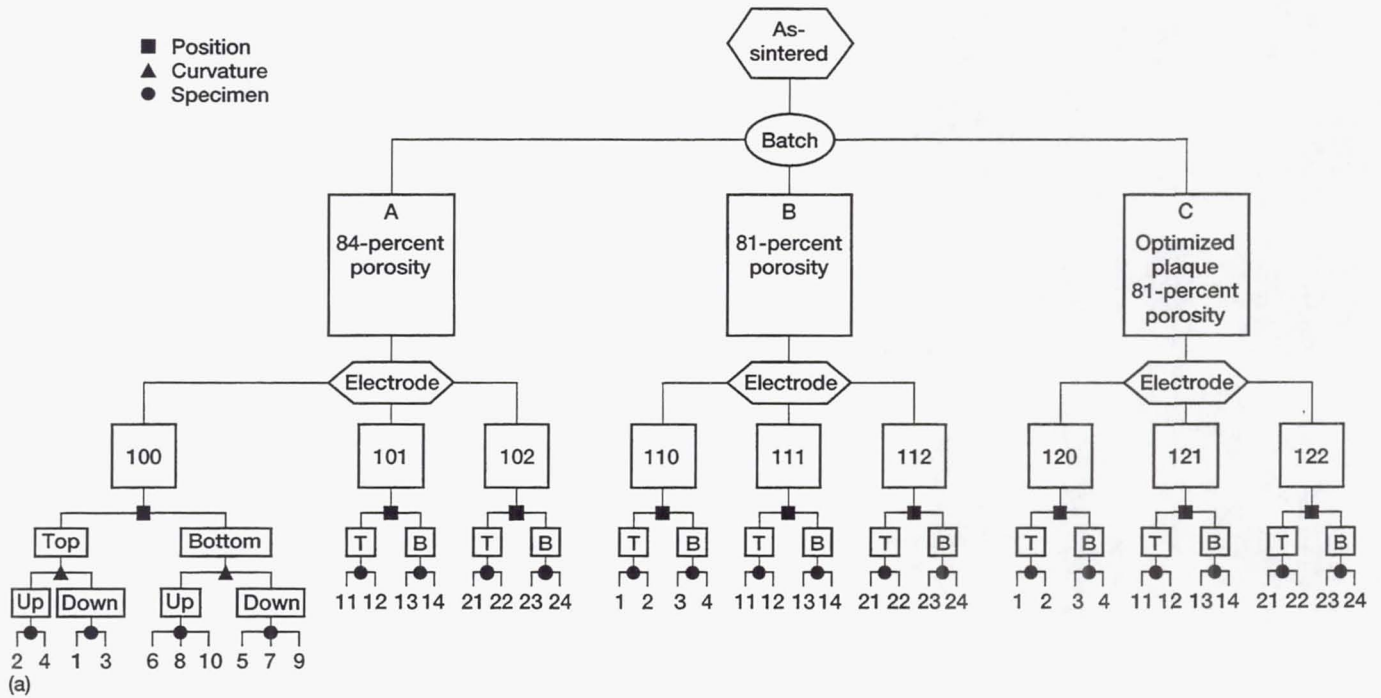


Figure 3.—Test matrix. (a) As-sintered electrodes. (b) Impregnated electrodes.

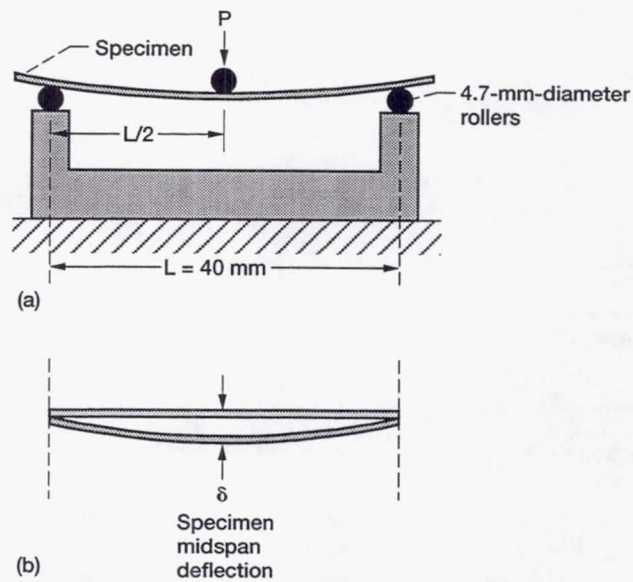


Figure 4.—Three-point bend fixture. (a) Schematic of fixture. (b) Specimen midspan deflection.

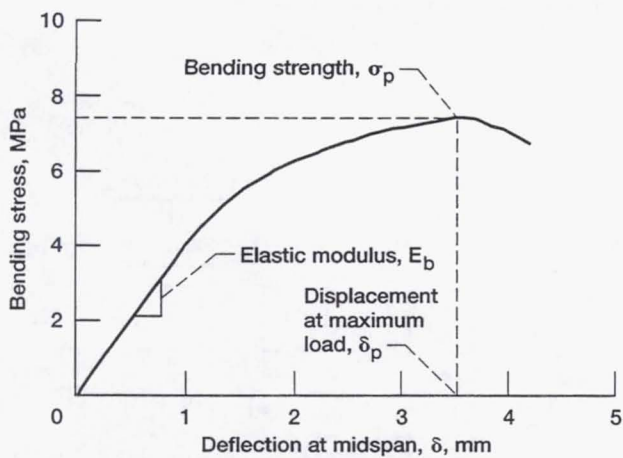


Figure 5.—Typical stress-displacement diagram showing critical measurements.

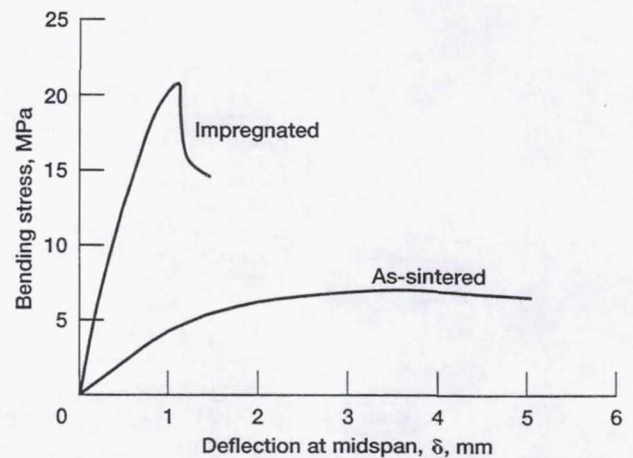


Figure 6.—Typical bending behavior of as-sintered and impregnated electrodes.

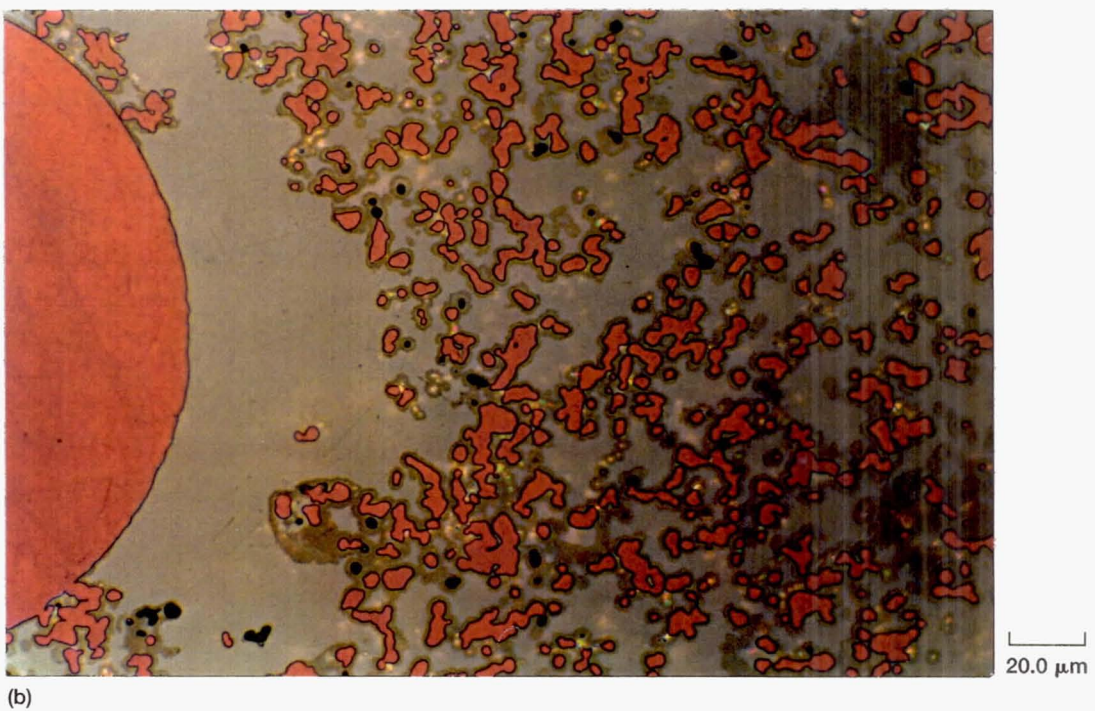
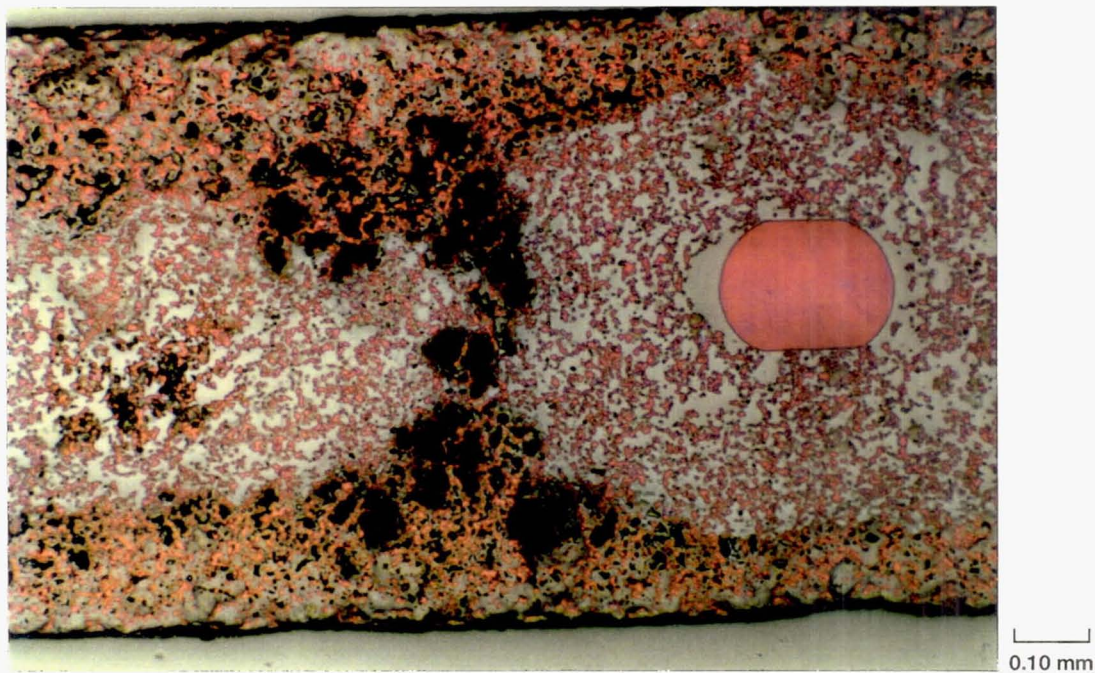


Figure 7.—Interference-layered electrode showing the various phases. (a) Surface loading is evident on each surface. (b)  $\text{Ni(OH)}_2$  coats most of Ni-powder particles, but not Ni-wire mesh.

**Page intentionally left blank**

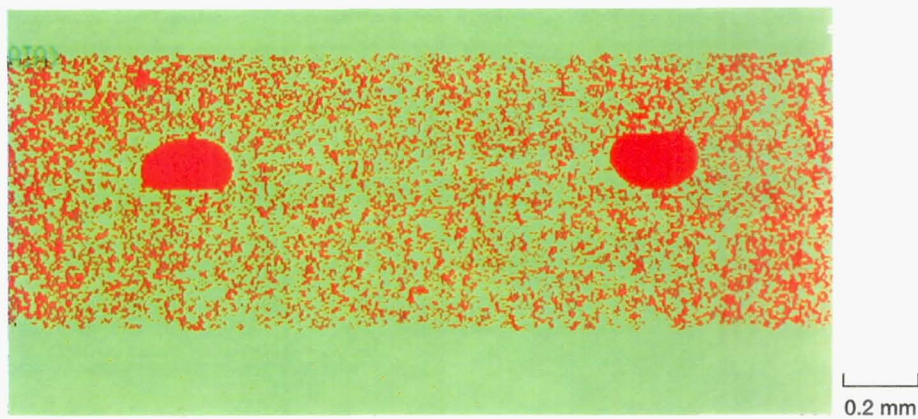
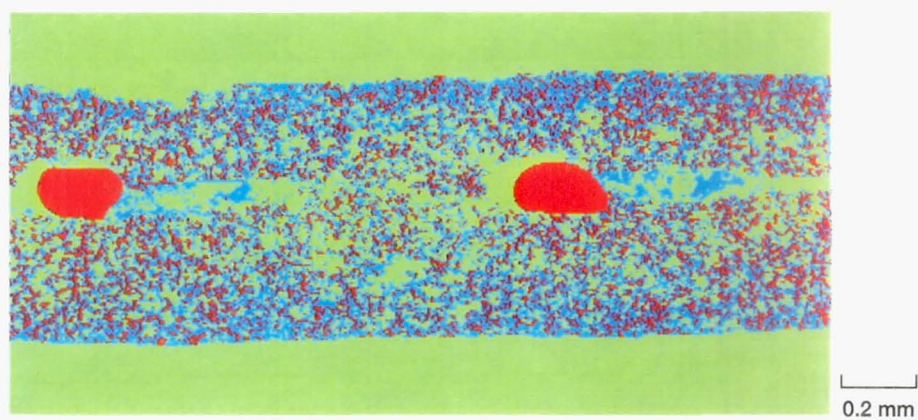
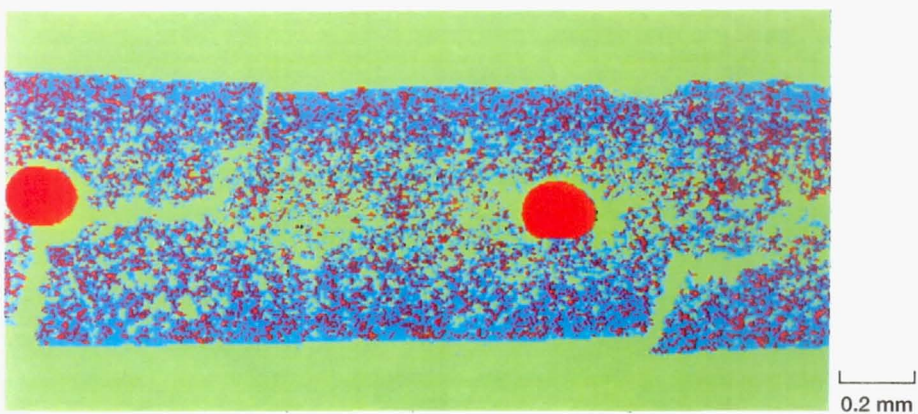


Figure 8.—Color-coded BSE image of batch C as-sintered electrode showing uniform distribution of Ni-powder (red phase).



(a)

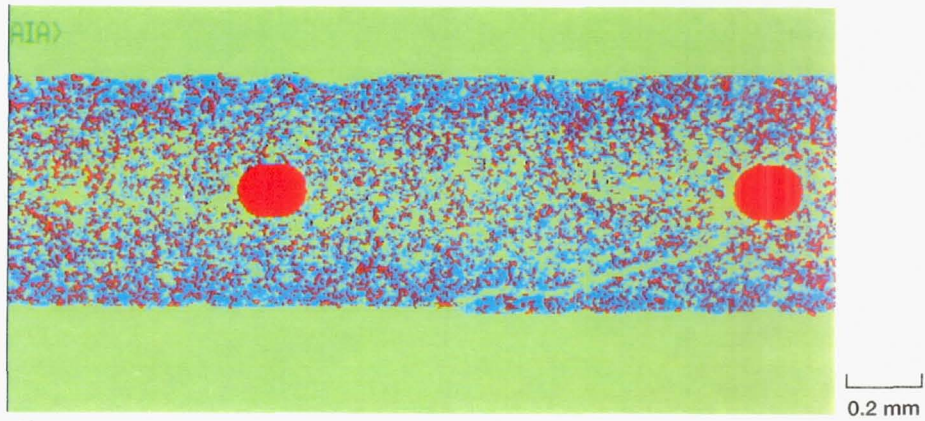


(b)

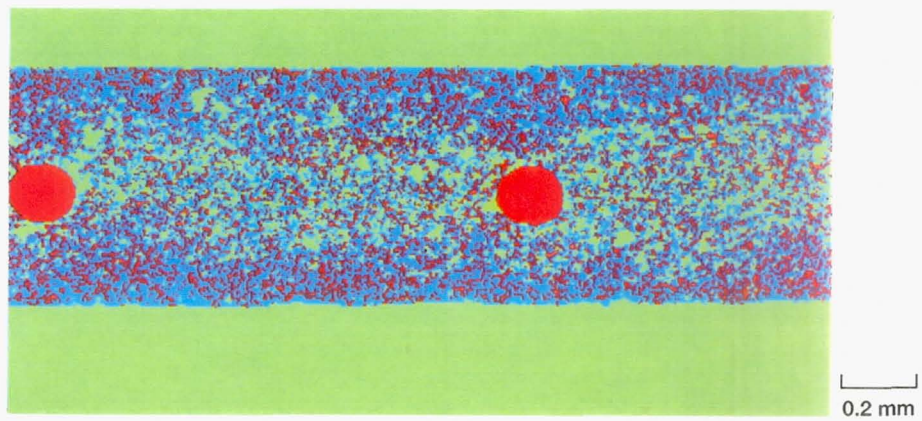
Figure 9.—Color-coded BSE images of batch A impregnated electrode s/n 202. (a) Taken from top of electrode. (b) Taken from bottom of electrode.



**Page intentionally left blank**



(a)



(b)

Figure 10.—Color-coded BSE images of batch A impregnated electrode s/n 200.  
(a) Taken from top of electrode. (b) Taken from bottom of electrode.

**REPORT DOCUMENTATION PAGE**Form Approved  
OMB No. 0704-0188

Public reporting burden for this collection of information is estimated to average 1 hour per response, including the time for reviewing instructions, searching existing data sources, gathering and maintaining the data needed, and completing and reviewing the collection of information. Send comments regarding this burden estimate or any other aspect of this collection of information, including suggestions for reducing this burden, to Washington Headquarters Services, Directorate for Information Operations and Reports, 1215 Jefferson Davis Highway, Suite 1204, Arlington, VA 22202-4302, and to the Office of Management and Budget, Paperwork Reduction Project (0704-0188), Washington, DC 20503.

1. AGENCY USE ONLY (Leave blank)		2. REPORT DATE January 1995	3. REPORT TYPE AND DATES COVERED Technical Memorandum	
4. TITLE AND SUBTITLE Bending Properties of Nickel Electrodes for Nickel-Hydrogen Batteries			5. FUNDING NUMBERS  WU-510-01-50	
6. AUTHOR(S) Brad A. Lerch, Richard M. Wilson, Dennis Keller, and Ralph Corner				
7. PERFORMING ORGANIZATION NAME(S) AND ADDRESS(ES) National Aeronautics and Space Administration Lewis Research Center Cleveland, Ohio 44135-3191			8. PERFORMING ORGANIZATION REPORT NUMBER  E-9178	
9. SPONSORING/MONITORING AGENCY NAME(S) AND ADDRESS(ES) National Aeronautics and Space Administration Washington, D.C. 20546-0001			10. SPONSORING/MONITORING AGENCY REPORT NUMBER  NASA TM-106756	
11. SUPPLEMENTARY NOTES Brad A. Lerch and Richard M. Wilson, NASA Lewis Research Center; Dennis Keller, Real World Quality Systems, Inc., 20388 Bonnie Bank Rocky River, Ohio 44116; and Ralph Corner, NYMA Inc., Engineering Services Division, 2001 Aerospace Parkway Brook Park, Ohio 44142 (work funded by NASA Contract NAS3-25266). Responsible person, Brad A. Lerch, organization code 5220, (216) 433-5522.				
12a. DISTRIBUTION/AVAILABILITY STATEMENT  Unclassified - Unlimited Subject Category 20			12b. DISTRIBUTION CODE	
13. ABSTRACT (Maximum 200 words)  Recent changes in manufacturing have resulted in nickel-hydrogen batteries that fail prematurely by electrical shorting. This failure is believed to be a result of a blistering problem in the nickel electrodes. In this study the bending properties of nickel electrodes are investigated in an attempt to correlate the bending properties of the electrode with its propensity to blister. Nickel electrodes from three different batches of material were tested in both the as-received and impregnated forms. The effects of specimen curvature and position within the electrode on the bending strength were studied, and within-electrode and batch-to-batch variations were addressed. Two color-imaging techniques were employed to differentiate between the phases within the electrodes. These techniques aided in distinguishing the relative amounts of nickel hydroxide surface loading on each electrode, thereby relating surface loading to bend strength. Bend strength was found to increase with the amount of surface loading.				
14. SUBJECT TERMS Bend tests; Electrodes; Nickel-hydrogen batteries; Strength; Modulus			15. NUMBER OF PAGES 19	
			16. PRICE CODE A03	
17. SECURITY CLASSIFICATION OF REPORT Unclassified	18. SECURITY CLASSIFICATION OF THIS PAGE Unclassified	19. SECURITY CLASSIFICATION OF ABSTRACT Unclassified	20. LIMITATION OF ABSTRACT	

National Aeronautics and  
Space Administration

**Lewis Research Center**  
21000 Brookpark Rd.  
Cleveland, OH 44135-3191

Official Business  
Penalty for Private Use \$300

POSTMASTER: If Undeliverable — Do Not Return